

# Performance Evaluation and Multidoped Composite Conditioned of A5-type/10% Ti-Sn Alloy: Processing and Properties

O. S. I. Fayomi · A. P. I. Popoola · F. Oyawale · O. O. Ajayi

Submitted: 25 September 2015 / Published online: 7 January 2016  
© ASM International 2016

**Abstract** The need to improve the mechanical and electrochemical performance of aluminum alloy for extended application is the motivation behind this present work which is the inoculation of  $\text{TiO}_2/\text{SnO}_2$  composite particulates on A500 by stir casting route. The effect of Ti/Sn on A500 aluminum series on the properties and microstructure of the produced alloy were investigated. The  $\text{TiO}_2/\text{SnO}_2$  was varied from 5 to 10 wt.%. The microstructural properties of these sequence alloys were investigated using scanning electron microscopy coupled with energy dispersive spectroscopy, and X-ray diffraction. The corrosion degradation properties in 3.65% NaCl solution were studied using linear potentiodynamic polarization technique. The wear and hardness of the composite-induced aluminum alloy were measured with dry abrasive MTR-300 testers and high diamond microhardness tester, respectively. The results showed that the average hardness value of 42.56 and 65.5 HV and wear loss of 1.5 and 0.5 g were obtained for the 0% and 10 wt.%  $\text{TiO}_2/\text{SnO}_2$  in A500 series. Hence, the addition of  $\text{TiO}_2\cdot\text{SnO}_2$  led to the precipitation and modification of complex intermetallic particles like  $\text{Al}_2\text{SnTiO}$  and  $\text{AlSiSn}$  which also indicate a fairly good interfacial interaction. This outcome has established that up to 10 wt.% particulate on A500 aluminum can be used in enhancing the tribology,

microhardness, and corrosion mitigation of aluminum alloy.

**Keywords** A5-type/Ti-Sn · Stir casting · Mechanical properties · Microstructure

## Introduction

The engineering role of aluminum to national growth and development both for industries and domestics are enormous. The widespread usage in various industrial capacities such as construction, automotive, and aircraft industries has made it suitable in recent time [1–8]. The demand has also been attested to be over twenty million of new aluminum products with no variance in superiority between virgin and reprocessed aluminum [1, 4–7]. Although they are softer in nature, possesses ductile behavior, with high electrical conductivity, and suitable corrosion resistant. The demand for higher strength, high corrosion resistance, and formability for ever-growing applications necessitate particle infringement [9–16]. In other words, extended and advantageous behavior for Al can be obtained with incorporation of particles by liquid stir cast method.

Particle infringement into liquid melt is known as Inoculation and is the addition of solid particles to a metallic melt to act as nucleate catalysts for the formation of fine equiaxed, rather than columnar grains [17]. Refiners or alloyed for aluminum are with copper, zinc, magnesium, manganese chromium, titanium, zirconium, lead, bismuth, nickel, and silicon [18]. Multiple matrix melts in the case titanium content often leads to rapid dissolution of the  $\text{Al}_3\text{Ti}$ , while the  $\text{TiB}_2$  remains stable. Magnesium particle

---

O. S. I. Fayomi (✉) · F. Oyawale · O. O. Ajayi  
Department of Mechanical Engineering, Covenant University,  
P.M.B 1023, Ota, Ogun State, Nigeria  
e-mail: ojosundayfayomi3@gmail.com;  
ojofayomi@covenantuniversity.edu.ng; fayomio@tut.ac.za

O. S. I. Fayomi · A. P. I. Popoola  
Department of Chemical, Metallurgical and Materials  
Engineering, Tshwane University of Technology, P.M.B. X680,  
Pretoria, South Africa

inclusion in cast bath has been reported to induce crack and foster corrosion initiation instead of improving metal stability [19, 20]. Nickel particle as a refiner for ferrous and nonferrous castings has been a subject of interest over years. Some reports have shown that this metal helps to promote the formation of passive films resulting in a reduction in corrosion rate [9, 21, 22]. Although grain refiners have been used to enhance aluminum alloy properties, the study of the corrosion resistance, mechanical, and morphological behavior is also very essential in evaluating the performance of the alloy behavior [23].

In most recent time, composites in the form of ceramics and oxides have found express entrance into material industries. Interestingly achievable properties which cannot be achieved by each component separately are often obtainable with matrix alloy. The use of additives is extremely important due to their influence on the growth and structure of the resulting melt in such a way that they provide influence in physical and mechanical properties of cast such as grain size, brightness, internal stress, pitting, and even chemical composition [24, 25]. In this study an attempt to fabricate and develop a structurally modified alloy that will work against mechanical and electrochemical deterioration with the help of A5-type/10%Ti-Sn was studied.

## Experimental Procedure

### Preparation of Substrate and Fabrication of Alloy

The nanoparticles used in this work are  $\text{TiO}_2/\text{SnO}_2$  powder. These particles are obtained from South Africa. The substrate used in this work is A500-type Al-Mg-Si alloy which

was obtained from aluminum tower, Ogun state, Nigeria; high-purity A500-type compositions as shown in Table 1. The equipment used in this work included molding box, cylinder, crucible, diamond hardness tester, polishing machine, scanning electron microscope, X-ray diffractogram, etc.

### Methods

300 g portion of A500 series were liquefied by an electric furnace under a protective nitrogen census environment. At optimum temperature of 700 °C,  $\text{TiO}_2\cdot\text{SnO}_2$  particles were inserted into the melt based on that described in Table 2 with varying concentrations. The process was allowed for about 2-3 min for proper admixing and precipitation during which the temperature was sustained for super heating to occur. The processed liquid melts were then poured into permanent cast iron mold which was pre-heated to about 200 °C. Portions of the alloyed sample were further taken for machining and sectioning using diamond cutting disk at 6 rpm. SEM/EDS and XRD were used to examine the structural properties and phase change, respectively. The electrochemical performance was observed with the help of linear polarization method.

### Structural Studies

The evolution of the alloys was characterized using Jeol JSM6510 Scanning Electron Microscopy build with Energy Dispersive Spectroscopy (SEM-EDS). The identify phase change was done using the Rigaku/Dmax 2200 pc automatic X-ray diffractometer with Cu target Ka radiation.

**Table 1** Spectrometer analyzer of the produced A500 aluminum series

Element	Al	Si	Mg	Fe	Cu	Mn	Ti	Cr
Composition, wt. %	Balance	0.45	0.50	0.22	0.03	0.03	0.02	0.03

**Table 2** Processing method and designation of samples

Sample	Admix	Bath composition
Blank	0	300 g A500 + O
1	5% $\text{SnO}_2$	300 g A500 + 5% $\text{SnO}_2$
2	10% $\text{SnO}_2$	300 g A500 + 10% $\text{SnO}_2$
3	5% $\text{TiO}_2$	300 g A500 + 5% $\text{TiO}_2$
4	10% $\text{TiO}_2$	300 g A500 + 10% $\text{TiO}_2$
5	10% $\text{TiO}_2$ + 10% $\text{SnO}_2$	300 g A500 + 10% $\text{TiO}_2$ + 10% $\text{SnO}_2$

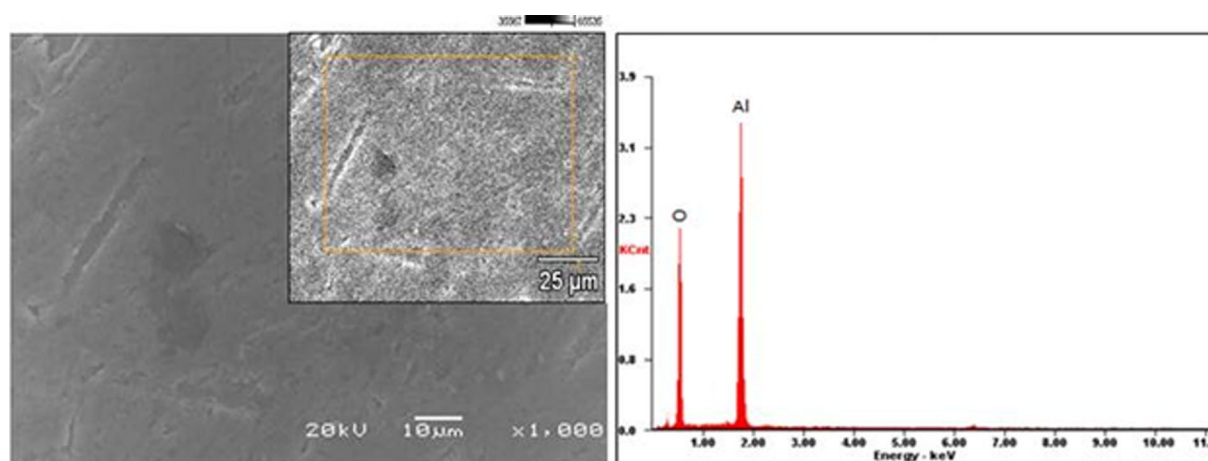


**Fig. 1** SEM/EDS morphology of A500 aluminum series

### Electrochemical Studies

Linear potentiodynamic polarization technique was used to verify the corrosion propagation in 3.65% NaCl solution at room temperature using Autolab data acquisition system model: AuT71791 and PGSTAT 30 with (GPES) package version 4.9. The polarization studies were determined from  $-1.5$  to  $+1.5$  V at a scan rate of  $0.003$  V/s. The saturated calomel electrode was used as a reference and graphite served as a counter electrode. An exposed area of  $1\text{ cm}^2$  with the alloy sample was used as working electrode.

### Microhardness Characterization

Microhardness of the fabricated alloys was examined using dura scan indenter microhardness tester. The indentations were taken along the surface of the alloyed sample using a load of  $10\text{ g}$  for  $10\text{ s}$  dwell time. The recorded values are an average of four serial measurements obtained from several locations.

### Tribological Characterization

MTR 300 dry abrasive rubber machine was used to examine the value of wear loss under dry silica sand as a wearing medium at a speed of  $100\text{ rev/min}$  for  $60\text{ s}$ . Both the initial and final mass loss was recorded. The obtained values were used to determine the percentage wear mass loss.

## Results and Discussion

The microstructure of as-received (cast Al without  $\text{TiO}_2$ - $\text{SnO}_2$ ) by SEM with EDS is shown in Fig. 1 with spectra indicating Al presence. The morphology of the working

metal indicates coarser and rather heterogeneous patches all over the sample. In Fig. 2, the effects of composite show reasonable uniform dispatches of the  $\text{SnO}_2$  and some macroresidual and segregation in some region. The effect of small percentage of  $5\%$   $\text{SnO}_2$  shows a well-harnessed Al-solidified precipitate at the surface. Though the strengthening effect was not as preferred as  $\text{TiO}_2$  single blend, reason being that  $\text{SnO}_2$  solute particles are expected to have oxidized to form blended clusters in the aluminum matrix.

The characteristics of sample 5 ( $10\%$   $\text{TiO}_2 + 10\%$   $\text{SnO}_2$ ) change due to Sn and Ti composite in the Al melts. The presence of Ti in the alloy is revealed showing possible evenly intermetallic phases. Although [1, 9] stated in their report that structures of reinforced alloy will help to determine the mechanical properties of that material. With the admixed melt of  $\text{TiO}_2$  concentrate for samples 3 and 4, a sound improvement was seen from other properties studied. This dendritic system is enclosed by the eutectoid precipitant of small Ti particles all through the interface with both 5 and  $10\%$  admixed. Agglomeration does not exist for  $\text{TiO}_2$  unlike that of  $\text{SnO}_2$  diffusion which might have initiated pitting and porosity. Therefore addition of  $10\%$   $\text{TiO}_2$  to the Al-Mg-Si alloy revealed a complex  $\text{TiO}_2$ -based intermetallic compound within the aluminum solid melt. In fact, since structural refinement takes place due to the reduction of grain size [1, 11], particles of Ti might facilitate refinement and improvement in mechanical properties.

Vander Boon [9] noted that the serviceability of material which is alloyed is quantified to a huge extent by the conditioning addition and the metallurgical processes engaged. Also, it has been attested to that refiners added to a melt cumulate in structural modifications resulting in the establishment of intermetallic complex compounds [1, 25]. Most interestingly is the change in structure of the binary

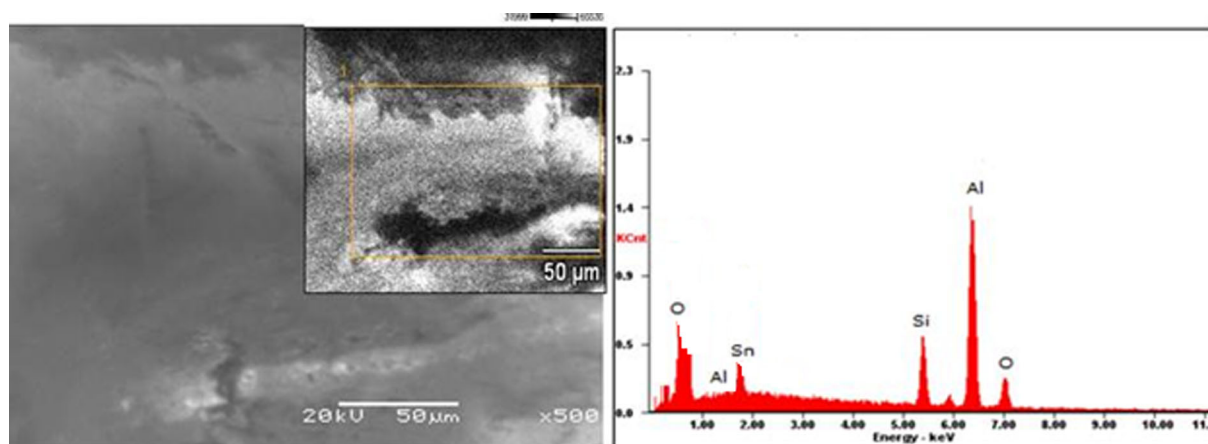


**Fig. 2** SEM/EDS morphology of 5%  $\text{SnO}_2$ -inoculated A500 aluminum series

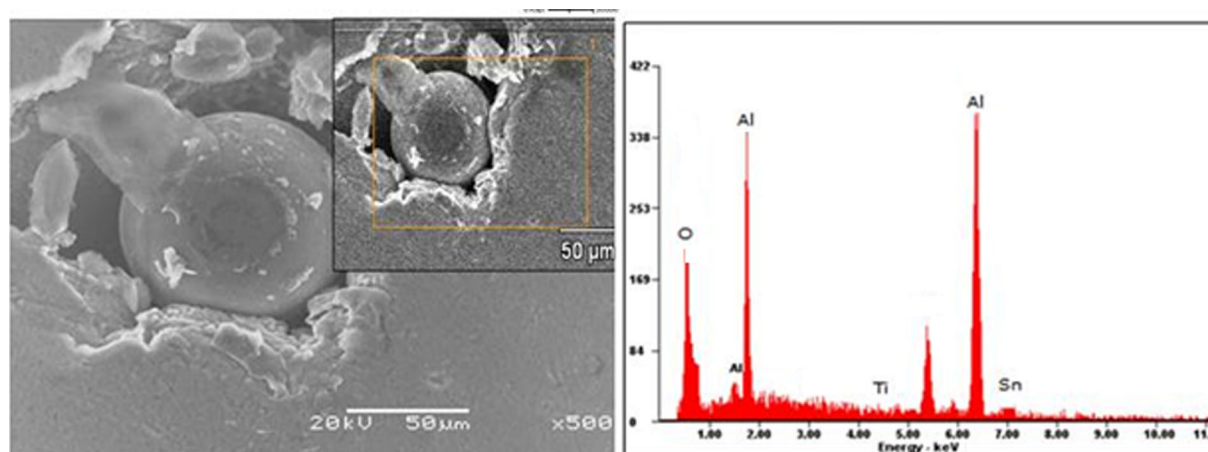


**Fig. 3** SEM/EDS morphology of 10 wt.%  $\text{TiO}_2/\text{SnO}_2$ -inoculated A500 aluminum series

composite admixed in Fig. 3 ( $\text{Al-Mg-Si} + 10\% \text{TiO}_2 + 10\% \text{SnO}_2$ ) with 10% each of the composite in the melt. Both functional particle of Ti and Sn were noticeable through EDX identification in appreciable quantity.

The XRD pattern of 5%  $\text{SnO}_2$ -inoculated A500 series is shown in Fig. 4. From Fig. 4 it was observed that the alloy had Al phase matrix of  $\text{AlSn}_2$ ,  $\text{Al}_2\text{Sn}_2$ , and  $\text{AlSn}_2\text{O}_{12}\text{Si}$ .  $\text{SnO}_2$  lumps and agglomeration causes microsegregation thus establishing eutectic within the zone [19]. In Fig. 5, more solid-bound alloy phase system of Ti/Sn matrix formation of complex intermetallic compounds was seen. The nucleation and wild spread of the composite particle-combined phase could be ascribed to the satisfactory sites for the nucleation offered by the aluminum particles that are formed on solidification.

According to [1, 9, 11], to enhance heterogeneous nucleation and achieve grain refinement, the nucleation substrates not only need to be potent, but also need to have an adequate proper particle size and a narrow size

distribution. In view of this, understanding the grain refinement attained by the liquid melt and the interfacial diffusion of the Ti/Sn composite can be well described in terms of their heterogeneous nucleation and phase bond as seen in Fig. 5 with Ti, Al;  $\text{SiTi}$ ,  $\text{AlSn}_2\text{O}_{13}\text{Ti}$ .

### Electrochemical Studies

Figures 6 and 7 show the polarization resistance and corrosion rate curve, respectively from linear potentiodynamic extrapolate data of all the conditioned alloys indicated in Table 2. The effect of composite particulate and their synergistic blend on as-cast alloy are seen from the potential/current trend. As-cast  $\text{Al-Mg-Si}$  alloy was used as control to other alloy-enhanced composite admixed melt. From observation, all particles inoculated provide good active-passive behavior except for 10%  $\text{SnO}_2$  (see Table 3). Although, literature attested that not all refiners or inoculant perform at their best on condition of

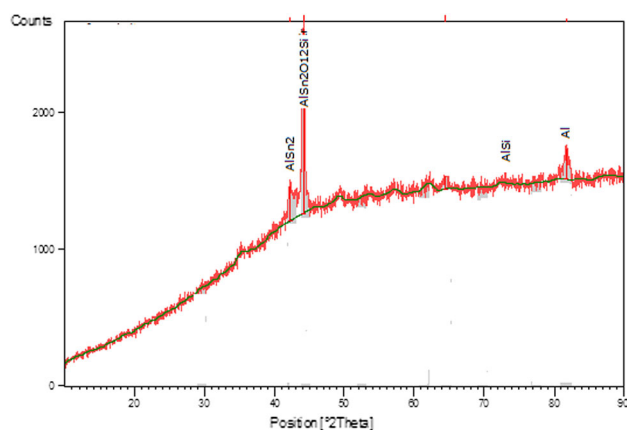


**Fig. 4** XRD pattern of 5% SnO<sub>2</sub>-inoculated A500-Al-Si

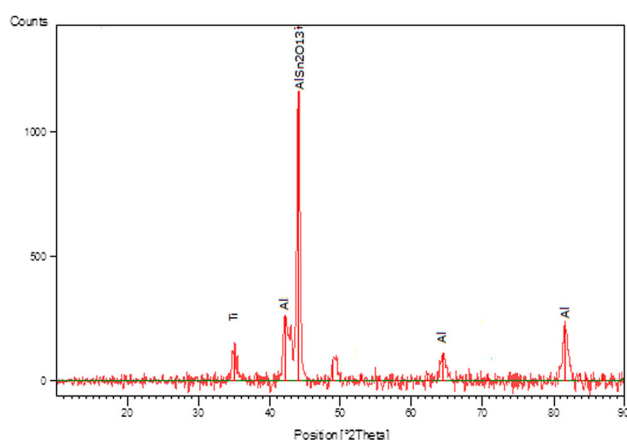


**Fig. 5** XRD pattern of 10% each of TiO<sub>2</sub>-SnO<sub>2</sub>-inoculated A500-Al-Si

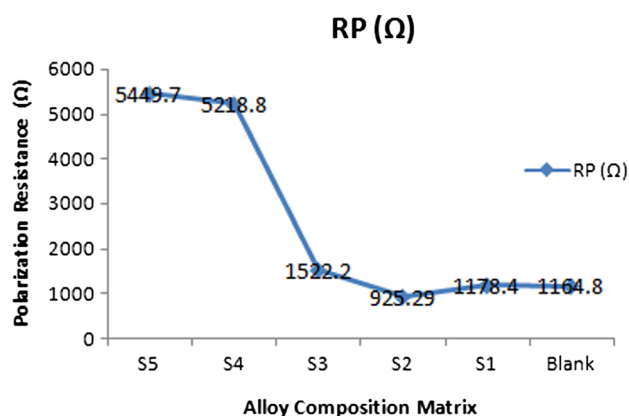


**Fig. 6** Linear potentiodynamic polarization trend (Polarization resistance/alloy composition) in 3.65% NaCl solution

application. In some case when intermediate precipitations are partly coherent with immediate matrix, defect tends to be obvious and provides such material-less polarization with current densities finding its way aggressively into the passive region.

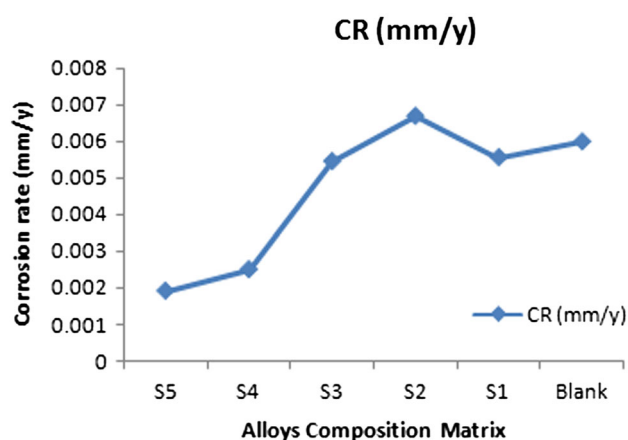


**Fig. 7** Linear potentiodynamic polarization curves for as-cast A500-Al-Si and TiO<sub>2</sub> (TiO<sub>2</sub>-SnO<sub>2</sub>) inoculated in 3.65% NaCl solution

In view of this, the influence of trace composite particulate and their synergistic blend on Al has great effect on the growth, nucleation, and the passivation potential as observed in Fig. 7. In other words, this behavior can be attributed to the perfect interaction, and the stability of this inoculant on the vacancies site. From the linear scan, the corrosion potential of the inoculated sample at 5% SnO<sub>2</sub> is  $-0.61085$  V, 10% SnO<sub>2</sub> is  $-0.65013$  V, 5% TiO<sub>2</sub> is  $-0.68609$  V, 10% TiO<sub>2</sub> is  $-0.79953$  V, 10% TiO<sub>2</sub>+10% SnO<sub>2</sub> is  $-0.6925$  V while that of as-cast Al is  $-0.85214$  V.

The corrosion rate (CR) follows the same trend. Sample 5 is  $0.001913$  mm/y, sample 4 is  $0.002503$  mm/y, sample 3 is  $0.005451$  mm/y, sample 2 is  $0.00669$  mm/y, sample 1 is  $0.00556$  mm/y, and  $0.00599$  mm/y for as-received sample. The decrease in deterioration behavior of the composite alloy was far encouraging with about four-time difference in magnitude ( $4.077 \times 10^{-3}$ ) when compared with control sample.

The best Rp value for the synergistic blend (10% TiO<sub>2</sub>-SnO<sub>2</sub>) was  $5449.7(\Omega)$  compared to that of as-received sample of  $1164.8(\Omega)$  as shown in Table 3.

In general, precipitation of two-phase Ti/Sn could be said to improve strength and corrosion stability. Although microconstituent has been affirmed to alter electrochemical corrosion process leading to non-uniform attached and initiation of corrosion region but in this study, reverse was the case. The magnitude of the dissolution does not depend on the percentage of the additive per say, but rather on the dispersion mechanism, and the activities of each constituent at the solid solution which help to stabilize the potential.

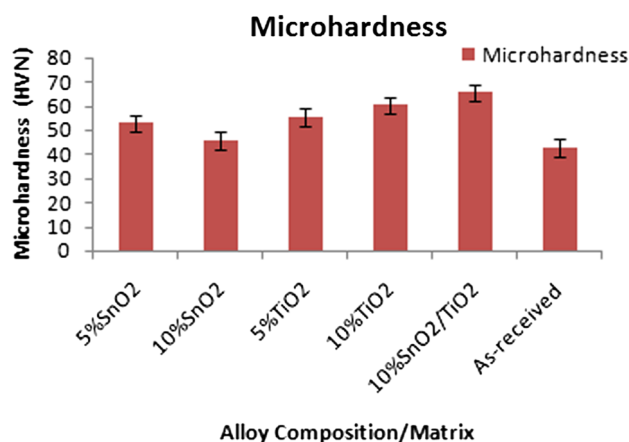
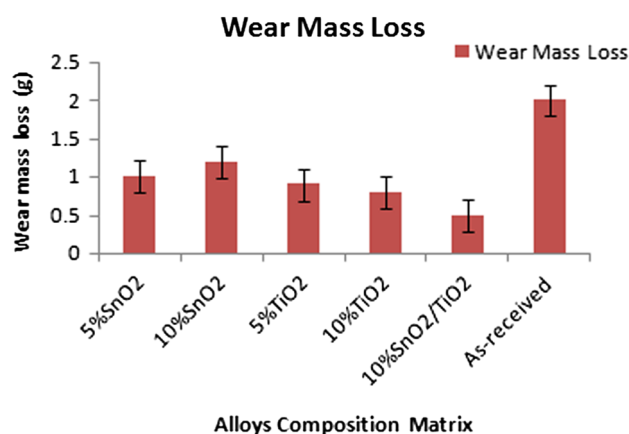
#### Wear/Microstructure Studies

Figures 8 and 9 present the microhardness and wear characteristics of as-received and conditioned alloy, respectively in their varied proportion. It is obvious that refiners play an



**Table 3** Potentiodynamic polarization data obtained from Tafel plot for as-cast Al-Mg-Si and alloyed Al-Mg-Si samples

Samples	$E_{\text{corr}}$ , V	$j_{\text{corr}}$ , A/cm <sup>2</sup>	$C_R$ , mm/y	$R_p$ , $\Omega$
S5	−0.69251	1.44E−06	0.001913	5449.7
S4	−0.79953	1.88E−06	0.002503	5218.8
S3	−0.68609	4.10E−06	0.005451	1522.2
S2	−0.65013	5.02E−06	0.00669	925.29
S1	−0.61085	4.17E−06	0.00556	1178.4
Blank	−0.85214	4.99E−06	0.00599	1164.8

**Fig. 8** Hardness behavior of as-received and conditioned alloys**Fig. 9** Wear mass loss of fabricated alloys

important role in the properties of the produced alloys. The microhardness (HVN) value of the Al-10TiO<sub>2</sub>-SnO<sub>2</sub> alloy gives a better hardness performance. From all indications, hardness increased from 42.56 HVN for base Al to approximately 65.5 HVN for Al-XTiO<sub>2</sub>-SnO<sub>2</sub> which is about 23.04 HVN significant improvements. The hardness characteristic followed the same trend with wear mass loss results with significant improved performance. Although the development of the composite particulate was primarily seen to have contributed immensely to the buildup of

substantial grain that forcibly retard the dislocation movement of the rig over the specimen. This accretion follows observation made by [24, 25]. The change in variation of the most performed alloy compared to the as-received alloy was twice improved. Another interesting fact is that oxide and composite has affinity to form solid precipitation and suitable interfacial diffusion which might result to fine-grained structure of the conditioned alloys. When this happened, the possibilities of retardation which will result to significant improved properties are accessed.

## Conclusion

- The A500/10 wt.%Ti-Sn metal alloys showed better dispersible characteristics than other added alloy refiner and as-received sample.
- All the aluminum series with composite particle addition improved significantly from 0 to 10 wt.%.
- The presence of intermetallic phases such as AlSn<sub>2</sub>Ti and Ti<sub>2</sub>SnAl<sub>6</sub> in the form of eutectic segment contributes immensely to the reduced wear deterioration, improved corrosion resistance, and promotes better hardness characteristics.
- Unalloy aluminum has been found to be unstable and unsuitable for use in a region with high corrosion environments.
- The addition of SnO<sub>2</sub>/TiO<sub>2</sub> particles to A500 aluminum series can be used to improve the mechanical and corrosion properties of the formed alloy.

**Acknowledgments** This work is supported through by Mr. Adelaja E.O of Covenant University. The financially support by the National Research Foundation, Pretoria, South Africa were deeply appreciated.

## References

1. Y. Chuang, S. Lee, H. Lin, Mater. Trans. **47**, 106 (2006)
2. M. Abdulwahab, A. Madugul, S.A. Yaro, S.B. Hassan, A.P.I. Popoola, Mater. Des. **32**, 1159 (2011)
3. N. Li, X. Lu, C. Jian-Zhong, Trans. Nonferrous Met. Soc. China **18**, 541 (2008)

4. F. Bonollo, J. Urban, B. Bonatto, M. Botter, *Metallurgiaitaliana* **6**, 23 (2005)
5. H.S. Ding, J. Gou, J and Jia. *J Trans. Nonferrous Met. Soc. China* **11**, 540 (2001)
6. J. Deshpande, Research Programs. Department of Manufacturing Engineering, Worcester Polytechnic Institute (2006).
7. O.P. Gbenedor, S.O. Adeosun, O.S.I. Fayomi, O.O. Joseph, *Int J. Sci. Eng. Res.* **3**, 2229–5518 (2012)
8. O.S.I. Fayomi, O.P. Gbenedor, M. Abdulwahab, C.A. Bolu, A.P.I. Popoola, *J. New Mater. Electrochem. Syst.* **16**, 059 (2013)
9. Vander Boon D. *Laboratory Module 3*, Grand Valley State University, (2005) pp. 1–5
10. Y. Wang, H.-T. Li, Z. Fan, *Trans. Indian Inst. Met.* doi:[10.1007/s12666-012-0194-x](https://doi.org/10.1007/s12666-012-0194-x)
11. A. Rashid, *The Treatment of Liquid Silicon–Aluminum Alloys*. Department of MME, BUET Dhaka (2010) lectures 17, chap. 7, pp. 1–15
12. M. Abdulwahab, I.A. Madugu, F. Asuke, O.S.I. Fayomi, F.A. Ayeni, *J. Mater. Environ. Sci.* **4**, 87 (2013)
13. L.A. Dobrzański, R. Maniara, J.H. Sokolowski, *J. Achiev. Mater. Manuf. Eng.* **17**, 217 (2006)
14. Nguyen H, School of Engineering, Grand Valley State (2005) 1
15. F. Grosselle, G. Timelli, F. Bonollo, R. Molin, *Metal Sci. Technol.* **22**, 2 (2009)
16. Sigworth C. K. *American Foundry Society* (2007) pp. 1–12
17. J. Szajnar, T. Wróbel, *J. Achiev. Mater. Manuf. Eng.* **27**, 95 (2008)
18. X. Bo, L. Yuandong, Y. Ma, H. Yuan, *China Foundry* **8**, 211 (2011)
19. R.Y. Chen, D. Willis, *J. Metall. Mater. Trans.* **36**, 117 (2005)
20. G.L. Dong, L. Kyuhong, K. Sunghak, *Surf. Coat. Technol.* **201**, 1296 (2006)
21. S. Yanwei, L. Bangsheng, L. Aihui, G. Jingjie, F. Hengzhi, *China Foundry* **7**, 43 (2010)
22. T. Ahmet, D. Mehmet, K. Sabri, *J. Mater. Sci.* **42**, 8298 (2007)
23. K. B. Rudman, *Metal Casting Reference Book*, Department of Materials Science and Engineering, Michigan Technical University, USA, (2005) p. 23
24. H. Ding, G. Zhou, D. Hui, (*Proc. IMechE*), Part J: Eng. Trib. **225**, 43 (2011)
25. O.P. Gbenedor, M. Abdulwahab, O.S.I. Fayomi, A.P.I. Popoola, *Chalcogenide Lett.* **9**, 201 (2012)